



RESEARCH MEMORANDUM

PRELIMINARY TANK INVESTIGATION OF THE USE OF SINGLE
MONOPLANE HYDROFOILS FOR HIGH-SPEED AIRPLANES

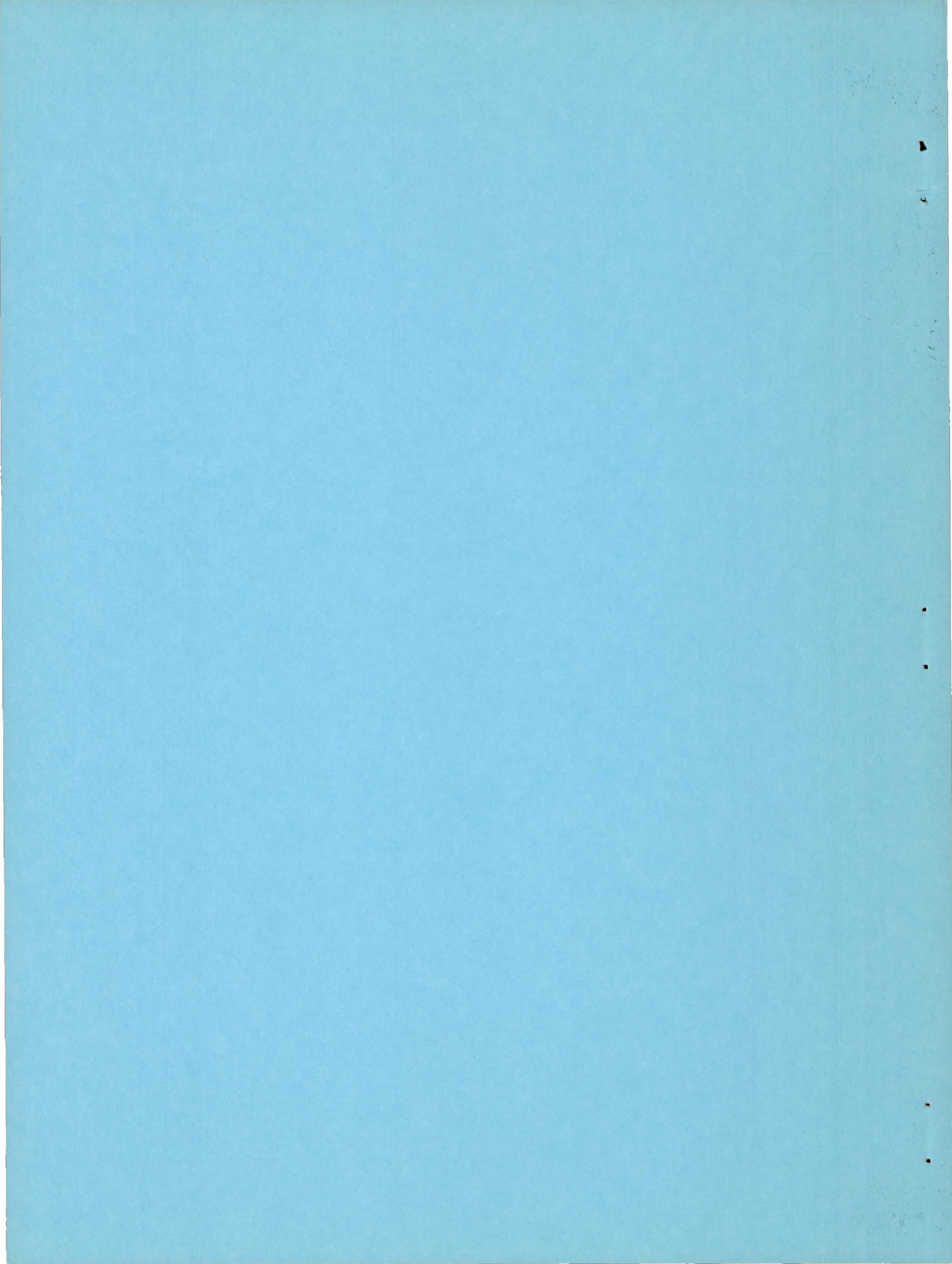
By

Douglas A. King and John A. Rockett

Langley Aeronautical Laboratory
Langley Air Force Base, Va.

NATIONAL ADVISORY COMMITTEE
FOR AERONAUTICS
WASHINGTON

March 22, 1949
Declassified August 18, 1954



NATIONAL ADVISORY COMMITTEE FOR AERONAUTICS

RESEARCH MEMORANDUM

PRELIMINARY TANK INVESTIGATION OF THE USE OF SINGLE
MONOPLANE HYDROFOILS FOR HIGH-SPEED AIRPLANES

By Douglas A. King and John A. Rockett

SUMMARY

A preliminary investigation was made in Langley tank no. 2 of the hydrodynamic take-off and landing characteristics of a $\frac{1}{12}$ -size model of a hypothetical jet- and rocket-propelled high-speed airplane fitted with various designs of a single monoplane hydrofoil mounted near the center of gravity. Instability of the airplane-hydrofoil combinations was present during a range of speed in which transition from hydrofoil action to planing-surface action of the hydrofoil occurred. With the best configurations the transition instability was reduced but none appeared acceptable for take-off. The maximum hump load-resistance ratio obtained was 2.67. Skipping occurred during landing with peak normal accelerations up to 4.4g. Breaker strips at the rear of the fuselage considerably improved the hydrodynamic characteristics.

INTRODUCTION

The feasibility of the water-based operation of high-speed airplanes is being investigated by the Langley Aeronautical Laboratory of the NACA. A dynamically similar model of a hypothetical jet- and rocket-propelled airplane is being used as a test vehicle and the effects of various modifications and types of water-landing gears on the take-off and landing characteristics are being studied (reference 1). The use of NACA hydro-skis in this connection has been reported in reference 2. The present paper describes a similar investigation of the use of hydrofoils as water-landing gear.

Numerous arrangements of hydrofoils have been proposed in the past for use on seaplanes and high-speed surface boats. Ladderlike arrangements were used successfully on seaplanes with a relatively low landing speed by Guidoni and on surface boats by Bell. Arrangements of monoplane hydrofoils intended to minimize the interference drag of the ladderlike systems have been proposed by Tietjens and Grunberg. The NACA has also investigated various hydrofoil systems on seaplanes and surface boats. A more extended discussion and references to original work can be found

in the section on hydrofoils in reference 3. As the lift-drag ratio of a submerged hydrofoil is greatly decreased by cavitation, a hydrofoil used as the water-landing gear of a high-speed airplane should preferably pass through the water surface and plane at a speed less than its cavitation speed.

Although a variety of hydrofoil systems is being considered, the preliminary tests were confined to single monoplane hydrofoils mounted near the center of gravity and stabilized when under water by the aft end of the fuselage. Six hydrofoils incorporating variations in area, plan form, dihedral, and section were included in the program.

Because of the inherent low air drag of the resulting configurations the hydrofoils were not designed with retraction in mind. In order to evaluate the effects on aerodynamic performance, wind-tunnel tests of a model similar to the tank model with and without one of the hydrofoils were made in the Langley 8-foot high-speed tunnel up to a Mach number of 1.2 (reference 4).

MODEL

The model used in the tank tests, designated as Langley tank model 229, was a $\frac{1}{12}$ -size dynamic model of a hypothetical transonic airplane of 13,140 pounds gross weight. It is fully described in reference 1 and is shown fitted with a hydrofoil in figures 1 and 2. The breaker strips shown on the model in figures 1 and 2 were used in all but the initial tests.

Other pertinent dimensions of the full-size airplane are given in the following table:

Weight in landing condition, pounds	8,720
Wing span, feet	25.0
Wing area, square feet	175
Length of fuselage, feet	42.22
Maximum diameter of fuselage, feet	5.0
Turbojet thrust, pounds	3,000
Rocket thrust, pounds	6,000
Moment of inertia in pitch, slug-feet ²	18,500
Moment of inertia in roll, slug-feet ²	2,440
Moment of inertia in yaw, slug-feet ²	15,600

The hydrofoils tested are shown in figure 3. Hydrofoils A and B had rectangular plan forms and 20° dihedral. The other hydrofoils had swept-back plan forms and 0° dihedral. Hydrofoil F was also tested with -10° and 30° dihedral. The areas and aspect ratios are noted on the figure. With the exception of hydrofoil D, all the hydrofoils were of polished

brass with 5-percent-thick plano-convex circular-arc sections for the hydrofoils and 10-percent-thick bicircular-arc sections for the struts. The plano-convex sections were used for ease of machining and also because the flat bottoms were considered to be preferable to the curved bottoms of airfoil sections for planing. Hydrofoil D was made of bismuth-tin alloy cast over a steel core with an NACA 63-010 section for the hydrofoil and an NACA 66-010 section for the strut.

Table I lists the position (designated by X, Y, and i as shown in fig. 1) of the hydrofoils, the length of the breaker strips measured from the rear end of the fuselage, and the type of tests made of each configuration. The distances X and Y are measured to the trailing edge of the hydrofoil center section from the nose and from the fuselage center line, respectively, and i is the incidence of the hydrofoil with respect to the fuselage center line, which was also the reference line for trim and angle of attack.

APPARATUS AND PROCEDURE

Tests were made in Langley tank no. 2 to determine the hydrodynamic take-off and landing characteristics of the model. The take-off tests were made by towing the model at various constant speeds, free to trim and rise, from the tank towing carriage. The take-off test setup is shown in figure 4. Resistance, trim, and rise of the center of gravity were measured, and photographs of the spray around the model were taken. The air drag of the towing gear was subtracted from the measured resistance, so that the resistance presented herein is the sum of the hydrodynamic resistance and air drag of the model. In the low-speed portions of the take-off tests the flaps were not deflected. Runs at high speeds, where the hydrofoil had lifted the wings clear of the water, were made with a flap deflection of 20° . An elevator deflection of 30° up was used for the take-off tests. The existence of porpoising was noted when present and was a factor in the progressive design of the various hydrofoils. No special investigation of the porpoising stability characteristics of the various configurations was made, however.

The landing tests were made by launching the model at several attitudes and speeds from the Langley tank no. 2 monorail and allowing the model to land on the water free of any restraint. All landings were made with the flaps deflected 20° . The speeds at which the model was launched during landing tests were determined from the aerodynamic characteristics of the model given in figure 5 of reference 1. The behavior of the model and length of the landing run were observed visually and photographically. Normal accelerations acting on the model were measured by a small spring-driven recording accelerometer mounted $8\frac{1}{2}$ inches forward of the center of gravity. Longitudinal decelerations were not measured by instrument but the mean longitudinal decelerations were computed from the observed lengths of landing runs.

The gross weight of the model for the take-off tests was 7.61 pounds (13,140 pounds, full-size). Landings were made at a gross weight of 5.05 pounds (8720 pounds, full-size), which corresponds to the weight of the airplane with most of the fuel expended.

RESULTS AND DISCUSSION

General Hydrodynamic Characteristics

The results of the hydrodynamic tests are given in figures 5 to 13 and tables II to VI in the form of pictures of the model during take-off and landing, plots of resistance, trim, and rise against speed, and tables of landing accelerations and length of landing run.

General behavior of model.- The hydrodynamic characteristics and behavior discussed in this section are those of the more nearly successful configurations, that is, the model with breaker strips on the fuselage and fitted with one of the large hydrofoils.

The take-off was characterized by several phases, which are illustrated by typical photographs of the model with hydrofoil C in figure 5. At rest the model floated at 0° trim with the center of gravity at the water line. At low speeds the bottom of the wing was in the water, and the fuselage acted as a displacement-type hull lifted upward by the submerged hydrofoil. A region of instability occurred in a speed range during which transition from hydrofoil action to planing-surface action of the hydrofoil occurred. At higher speeds the hydrofoil plane~~d~~ on the surface of the water. Many of the configurations ran steadily at these high speeds but porpoising occurred with some. The porpoising resembled upper-limit porpoising of seaplane hulls in that both the hydrofoil and the rear of the fuselage were involved.

For all of the hydrofoils except hydrofoil A the speed at which the hydrofoil emerged from the water was so low that cavitation should not occur on the full-size hydrofoil. The elevators produced enough moment to alter the trim appreciably, only at speeds greater than about 24 feet per second, model size.

In general, the landing run consisted of a series of fairly long, low skips that gradually decreased in magnitude as the model progressed along the landing run. The run was straight and very little change in attitude occurred during the skips. As the speed decreased to a low value near the end of the landing run the lift of the planing hydrofoil was no longer enough to support the load and the hydrofoil submerged. This drop of the model into the water occurred smoothly, with no trace of the transition instability noted during take-offs. Sequence photographs of a typical landing run are shown in figure 6. All of the configurations with breaker strips had similar landing characteristics.

Transition stability.- All of the hydrofoil systems exhibited a characteristic instability in a speed range during which transition from hydrofoil action to planing-surface action of the hydrofoil occurred. Model behavior in this range was a cyclical motion passing through the following steps in about 1 second:

- (a) Model running at low trim and rise with hydrofoil submerged.
- (b) Trim and rise increase slowly for a short time with hydrofoil submerged.
- (c) Trim and rise increase quite rapidly, the model pivoting about the rear end of the fuselage, until the flow separates over the top of the hydrofoil or the hydrofoil breaks through the water.
- (d) The hydrofoil loses lift and the model falls back to the position of stage (a).

Successive cycles occurred at intervals of about 3 to $3\frac{1}{2}$ seconds.

At the higher speeds of the range, the increase in rise and trim was so violent that the hydrofoil came completely out of the water. At the lower speeds the loss of lift of the hydrofoil was probably caused by a combination of flow separation and ventilation. Photographs of the model at low and high positions in the transition speed range are shown in figure 5.

The transition instability appears to be caused primarily by the changes in lift associated with passing through the free-water surface from a hydrofoil condition to a planing-surface condition (reference 5). It has also been suggested that the instability is aggravated by the proximity and shape of the fuselage bottom.

Deflecting the flaps had been found to lower the trim at low speeds where the flaps were in the water. It was thought that transition instability could be overcome by holding down the trim in this manner, decreasing the lift of the submerged hydrofoil, until a speed was reached at which the planing hydrofoil would support the model. This procedure was tried but was unsuccessful. With the flaps down, transition instability was more violent. Making accelerated runs at about 2 or $2\frac{1}{2}$ feet per second per second through the speed range for transition instability resulted in only a slight alleviation of the instability.

Although the transition instability of configurations incorporating sweep, low aspect ratio, and 0° dihedral was less severe than that of other configurations, none of them appeared to be sufficiently stable to allow acceptable take-offs.

Resistance.- The resistance of the model with any of the hydrofoils was greater in proportion to the weight than that of conventional sea-plane floats. The lowest hump resistance obtained in the tests was that of the model with hydrofoils C at $X = 20$ inches, $Y = 4.5$ inches, and $i = 2^\circ$. (See fig. 13(c).) For this configuration the gross load-resistance ratio at the hump was 2.67, as compared to 4 or more for conventional hulls. This high resistance, however, is probably acceptable in view of the low power loadings of such high-speed airplanes and the ease of adding auxiliary thrust units for take-off.

Breaker strips.- Take-off characteristics of the model with hydrofoil A with and without breaker strips extending 18 inches forward of the stern are shown in figure 7. Without the breaker strips the model porpoised severely with the rear of the fuselage fairly deep in the water and had an accompanying high resistance. The porpoising appeared at speeds just greater than the range of speeds in which transition from hydrofoil action to planing-surface action of the hydrofoil occurred. Installing the 18-inch breaker strips reduced the tendency of the stern to be sucked into the water, reduced the resistance, and deferred porpoising to a much higher speed. The 18-inch breaker strips were also used in the tests of hydrofoil B, but for the remainder of the tests breaker strips extending to the nose of the model were installed since this also eliminated spray in the vicinity of the turbojet air intakes at low speeds, as shown in figure 5. The results of reference 6 indicate that smaller strips could be used without having spray enter the intakes.

Development of Hydrofoils

The full-size speed at which hydrofoil A passed through the water surface and began to plane was approximately its cavitation speed. Hydrofoil B, having twice the area of hydrofoil A, was next tested on the model. The effect on take-off characteristics of doubling the hydrofoil area is shown in figure 8. As can be seen, the large hydrofoil B caused the model to rise in the water at lower speed and resulted in lower hump resistance than the smaller hydrofoil A. The resistance characteristics at high planing speeds were approximately the same with both hydrofoils. At high speeds the model porpoised with both hydrofoils. During this porpoising the model pivoted about the planing hydrofoil with little vertical movement of the center of gravity.

It was thought that the short over-all length of hydrofoils A and B may have been a factor in the porpoising experienced because of the correspondingly short restoring travel of the center of pressure. Accordingly, the total length of the remaining hydrofoils was increased by introducing sweep. The take-off characteristics of the model with hydrofoils B and C are compared in figure 9. Photographs of the spray of the model with hydrofoil C are given in figure 5. Porpoising at high speeds was not encountered with hydrofoil C. The speed at which transition instability started and the range of speed in which it occurred were less with hydrofoil C than with hydrofoil B.

When the model was fitted with hydrofoil D, which had a symmetrical, low-drag, airfoil section, transition instability occurred over a large speed range and the model was unstable at planing speeds, as shown in figure 10.

Results of the take-off tests of the model fitted with hydrofoil E, which had an aspect ratio of 1, are given in figure 11. The range of speed during which transition instability occurred was about the same as that of the model with hydrofoil C, but the instability was less severe. The normal accelerations experienced by the model during landing were less when it was fitted with hydrofoil E than with hydrofoil C (tables IV and V). Extension of the investigation to hydrofoils of lower aspect ratio was not considered to be too useful as it would lead to shapes approximately those of hydro-skis, which had already been investigated.

Effects of Some Hydrofoil Parameters

Hydrofoil dihedral.- Since hydrofoils having either dihedral or sweep alone had exhibited transition instability, the effect of dihedral on the swept hydrofoil F was investigated. The results are given in figure 12. As can be seen, hydrofoil F with zero dihedral was the most satisfactory, as hydrofoil F with -10° and 30° dihedral had large speed ranges in which transition instability and porpoising occurred.

Results of the landing tests of the model with hydrofoil F at 30° dihedral are given in table VI, and sequence photographs and a time history of normal accelerations during a typical landing are given in figure 6. The accelerations experienced during landings by the model fitted with hydrofoil F at 30° dihedral were slightly greater than those with hydrofoils C and E.

Hydrofoil position.- The effects on take-off characteristics of the longitudinal position, vertical position, and incidence of the hydrofoil are shown for the model fitted with hydrofoil C in figure 13. In general, similar tests of the model with other hydrofoils showed comparable effects.

As shown in figure 13(a), moving the hydrofoil rearward decreased the planing resistance and lowered the trim. There was no effect on the range of speed in which transition instability occurred. In general, moving the hydrofoil aft also decreased the normal accelerations and longitudinal decelerations experienced during landings. (See tables III, V, and VI.) However, when the hydrofoil was too far aft, the model tended to dive after landing, as indicated by the results given in table VI of landing tests for hydrofoil F with 30° dihedral.

Increasing the vertical distance between the fuselage and hydrofoil increased the trim and rise of the center of gravity at planing speeds and increased the hump resistance, as shown in figure 13(b).

Variation of the hydrofoil incidence had very little effect on the resistance at planing speeds, although increasing the incidence lowered the trim and slightly increased the rise. Figure 13(c) shows that the greatest effect of hydrofoil incidence was on the speed at which transition instability started and on hump resistance. Increasing the incidence increased the hump resistance and lessened the speed at which transition instability started. The minimum speed range in which transition instability occurred was with 2° incidence. The hydrofoil incidence had little effect on the accelerations experienced during landings.

CONCLUSIONS

On the basis of preliminary hydrodynamic tests of a model of a high-speed airplane fitted with a single monoplane hydrofoil the following conclusions were drawn:

1. All configurations tested exhibited a characteristic instability during a range of speed in which transition from hydrofoil action to planing-surface action of the hydrofoil occurred. The transition instability was made less severe by varying hydrofoil parameters, but none of the configurations appeared to be acceptable for take-off.

2. The hydrodynamic resistance of the model fitted with a hydrofoil was greater in proportion to the weight than that of conventional sea-planes. The maximum hump load-resistance ratio obtained was 2.67.

3. A typical landing run consisted of a series of low skips, with peak normal accelerations of from 2.1g to 4.4g, and mean longitudinal decelerations of from 0.24g to 0.45g.

4. Fitting breaker strips at the rear of the fuselage considerably improved the hydrodynamic characteristics.

Langley Aeronautical Laboratory
National Advisory Committee for Aeronautics
Langley Air Force Base, Va.

REFERENCES

1. King, Douglas A.: Tests of the Landing on Water of a Model of a High-Speed Airplane - Langley Tank Model 229. NACA RM No. L7I05, 1947.
2. Dawson, John R., and Wadlin, Kenneth L.: Preliminary Tank Tests of NACA Hydro-Skis for High-Speed Airplanes. NACA RM No. L7I04, 1947.
3. Benson, James M., and Bidwell, Jerold M.: Bibliography and Review of Information Relating to the Hydrodynamics of Seaplanes. NACA ACR No. L5G28, 1945.
4. Wood, Raymond B.: Effects of a Sweptback Hydrofoil on the Force and Longitudinal Stability Characteristics of a Typical High-Speed Airplane. NACA RM No. L8I30a, 1948.
5. Benson, James M., and Land, Norman S.: An Investigation of Hydrofoils in the NACA Tank. I - Effect of Dihedral and Depth of Submersion. NACA ACR, Sept. 1942.
6. Wadlin, Kenneth L., and Ramsen, John A.: Tank Spray Tests of a Jet-Powered Model Fitted with NACA Hydro-Skis. NACA RM No. L8B18, 1948.

TABLE I

SUMMARY OF CONFIGURATIONS TESTED AND TYPES OF TESTS MADE

Hydrofoil	Dihedral (deg)	Hydrofoil position			Length of breaker strips (in.)	Tests made	
		X (in.)	Y (in.)	i (deg)		Take-off	Landing
A	20	19	5.5	5	0		*
		19.5	5.5	5	0		*
		20	4.5	2	0	*	*
				2	18	*	
				5	18	*	
		5.5	2	0		*	
B	20	20	4.5	5	18	*	
C	0	19	4.5	5	41	*	
		20	3.9	5	41	*	
			4.5	0	41	*	
			2	41	*	*	
		5	41	*	*		
		5.5	5	41	*		
D	0	20	4.5	5	41	*	
E	0	20	4.5	2	41		*
				5	41	*	*
		21	4.5	2	41		*
F (-10° (0°) (30°)	-10	20	4.5	5	41	*	
	0	20	4.5	5	41	*	
	30	20	4.5	5	41	*	*
		21	4.5	5	41		*

TABLE II
EFFECT OF VARIOUS MODIFICATIONS ON LANDING CHARACTERISTICS OF MODEL 229

Modification	Attitude (deg)	Speed (full-size) (mph)	Peak normal acceleration (g)	Longitudinal deceleration		Length of run, (full-size) (ft)
				Peak (g)	Mean (g)	
No modification (reference 1)	8	141	7.4		1.05	630
	12	124	6.0		.77	690
Planing surface at rear of fuselage (reference 1)	8	141	4.6	3.6	1.21	550
	12	124	4.8	3.6	.82	650
NACA hydro-skis (reference 2)	8	141	2.0	.5	.28	2400
Hydrofoil A(a) position 20/5.5/2 (b)	8	141	3.6		.39	1680
	12	124	4.4		.44	1200
Hydrofoil C position 20/4.5/5	8	141	3.2		.25	2680
	12	124	3.6		.29	1850
Hydrofoil E position 20/4.5/5	8	141	2.1		.29	2280
	12	124	3.4		.33	1620
Hydrofoil F with 30° dihedral position 20/4.5/5	8	141	3.3		.37	1780
	12	124	4.0		.38	1390

Notes

(a) Without breaker strips.

(b) Position numbers refer to longitudinal position, X; vertical position, Y; and incidence, i.

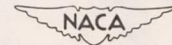


TABLE III

SUMMARY OF RESULTS OF LANDING TESTS OF MODEL WITH
HYDROFOIL A AND WITHOUT BREAKER STRIPS

12

Hydrofoil position			Attitude (deg)	Speed, full-size (mph)	Peak normal acceleration (g)	Mean longitudinal deceleration (g)	Length of run, full-size (ft)
Longitudi- nal, X (in.)	Vertical Y (in.)	Incidence, i (deg)					
19	5.5	5	8	141	4.8	0.39	1680
			12	124	5.1	.45	1150
19.5	5.5	5	8	141	4.6	.48	1200
			10	131	5.4	.40	1440
			12	124	5.8	.40	1320
20	4.5	2	8	141	2.6	.48	1320
			12	124	2.2	.76	700
20	5.5	2	8	141	3.6	.39	1680
			10	131	4.2	.39	1470
			12	124	4.4	.44	1200

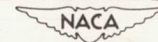


TABLE IV

SUMMARY OF RESULTS OF LANDING TESTS OF MODEL WITH HYDROFOIL C

Hydrofoil position			Attitude (deg)	Speed, full-size (mph)	Peak normal acceleration (g)	Mean longitudinal deceleration (g)	Length of run full-size (ft)
Longitudinal, X (in.)	Vertical, Y (in.)	Incidence, i (deg)					
20	4.5	-2	8	141	3.0	0.28	2400
20	4.5	5	8	141	3.2	.25	2680
			12	124	3.6	.29	1850

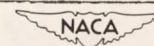


TABLE V

SUMMARY OF RESULTS OF LANDING TESTS OF MODEL WITH HYDROFOIL E

Hydrofoil position			Attitude (deg)	Speed, full-size (mph)	Peak normal acceleration (g)	Mean longitudinal deceleration (g)	Length of run, full-size (ft)
Longitudinal, X (in.)	Vertical, Y (in.)	Incidence, i (deg)					
20	4.5	2	8	141	2.6	0.30	2220
			12	124	2.9	.26	2040
20	4.5	5	8	141	2.1	.29	2280
			12	124	3.4	.33	1620
21	4.5	2	8	141	2.9	.30	2200
			12	124	3.5	.24	2250



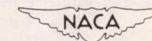
TABLE VI

SUMMARY OF RESULTS OF LANDING TESTS OF MODEL WITH HYDROFOIL F

WITH 30° DIHEDRAL

Hydrofoil position			Attitude (deg)	Speed full-size (mph)	Peak normal acceleration (g)	Mean longitudinal deceleration (g)	Length of run, full-size (ft)
Longitudinal, X (in.)	Vertical, Y (in.)	Incidence, i (deg)					
20	4.5	5	8	141	3.3	0.37	1780
			12	124	4.0	.38	1390
21	4.5	5	8	141	3.0	^a 1.10	600
			12	124	3.7	^a .76	700

(a) Model tended to dive.



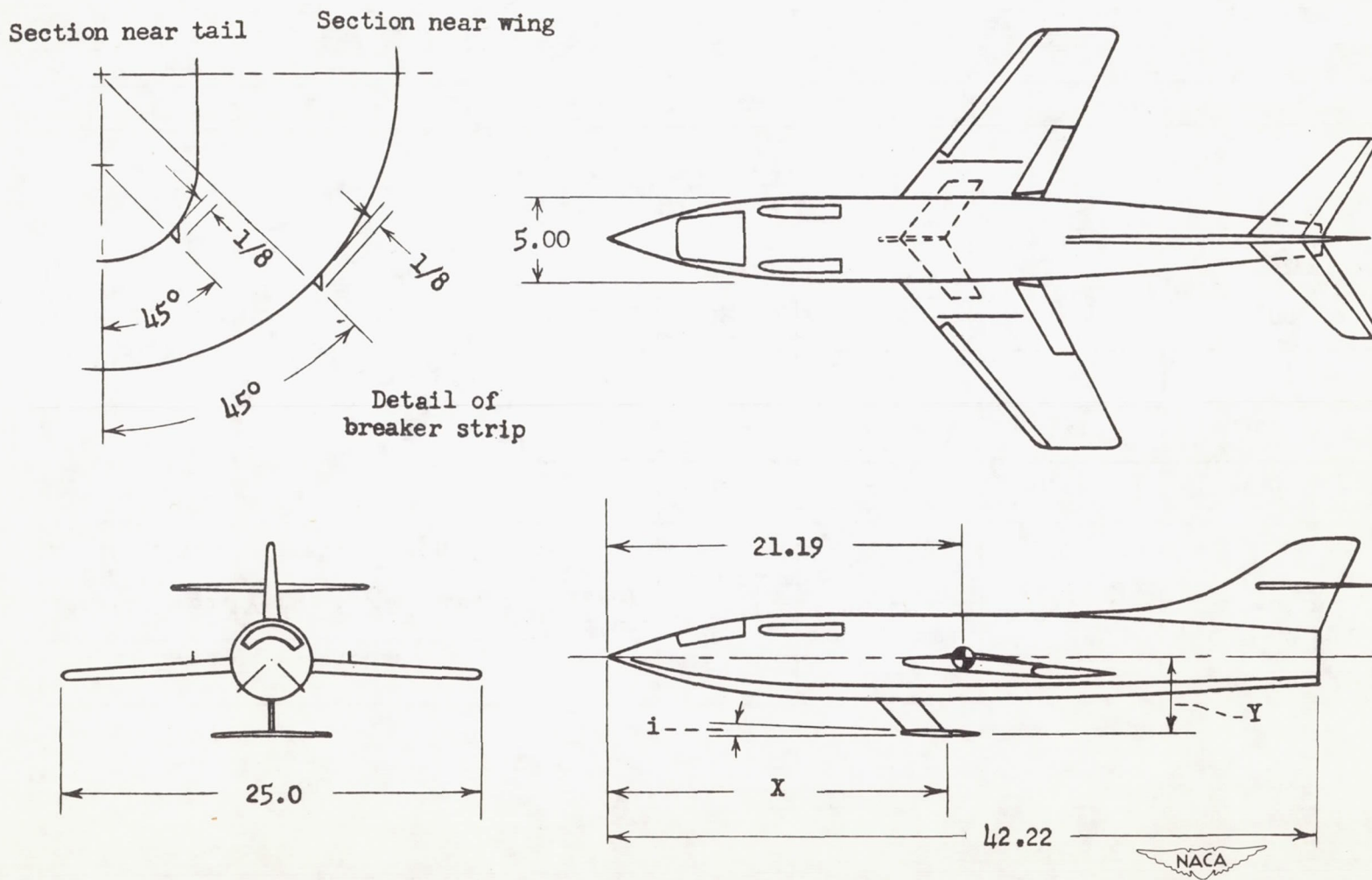


Figure 1.— General arrangement of model 229 with hydrofoil D. (All dimensions are feet full-size, inches model size.)

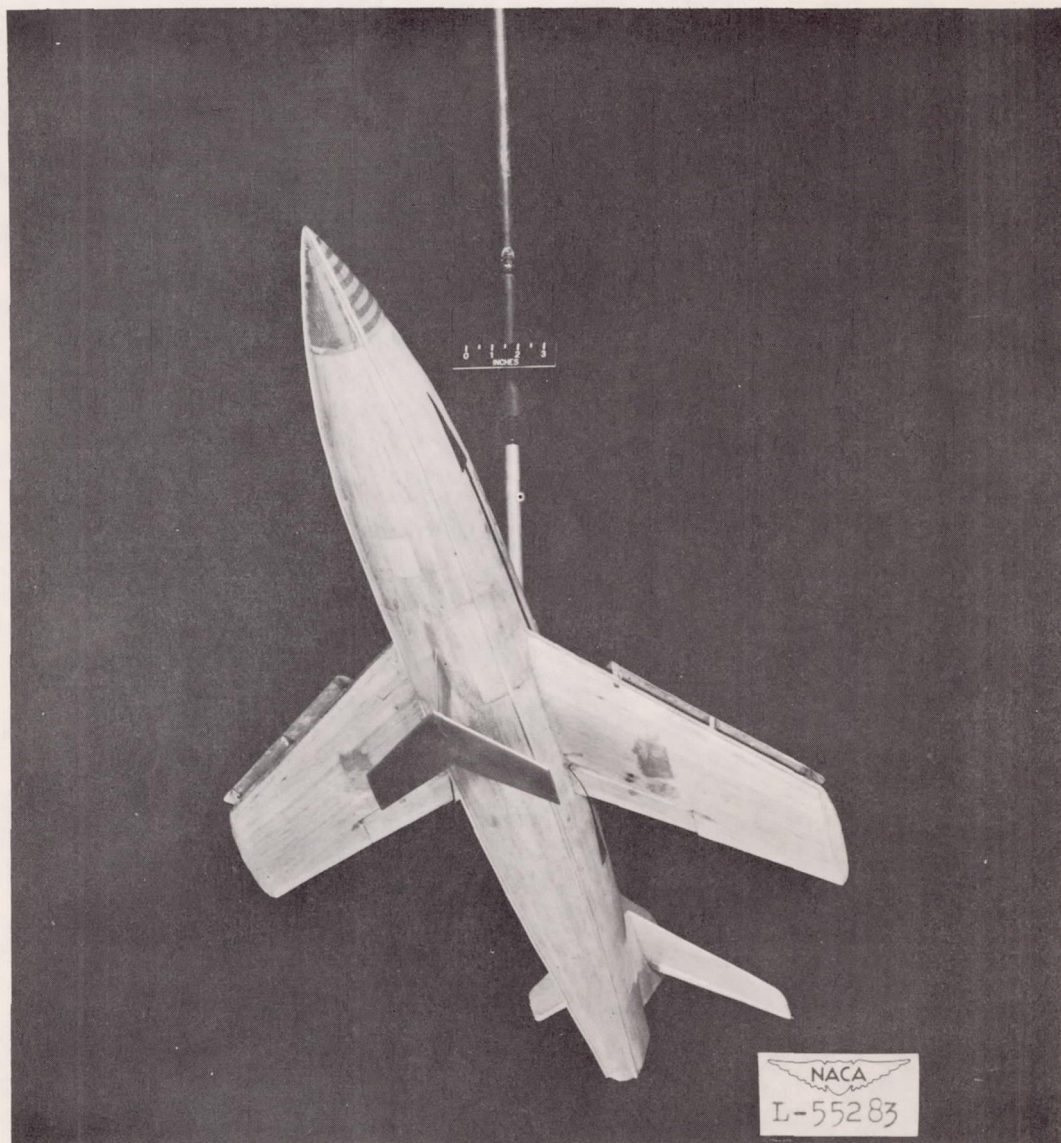
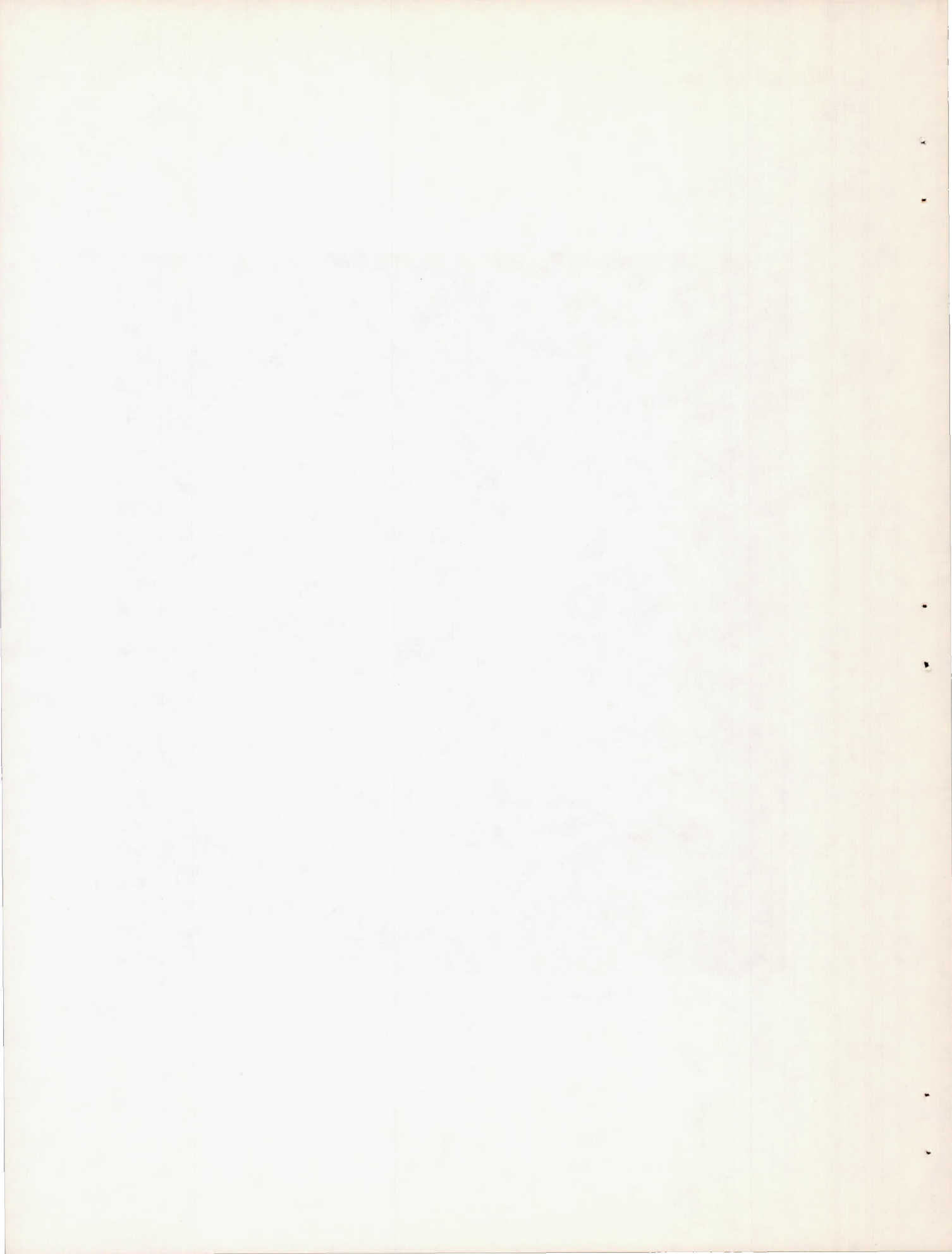


Figure 2.— Photograph of model 229 with hydrofoil D.



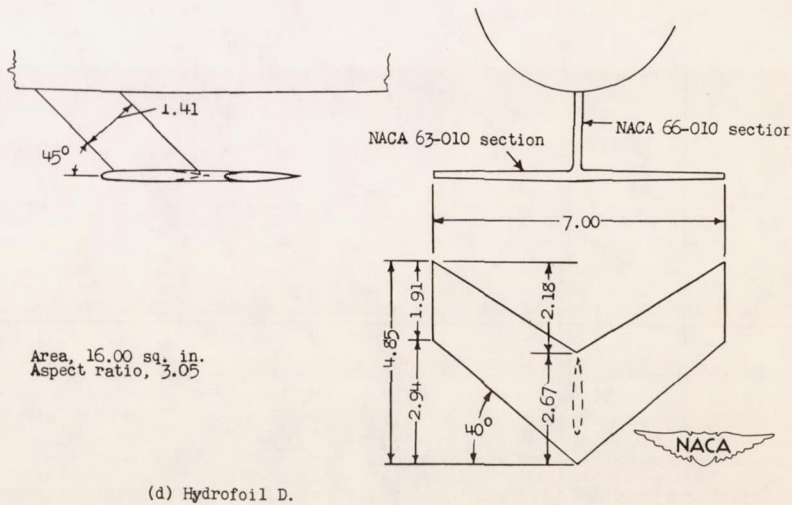
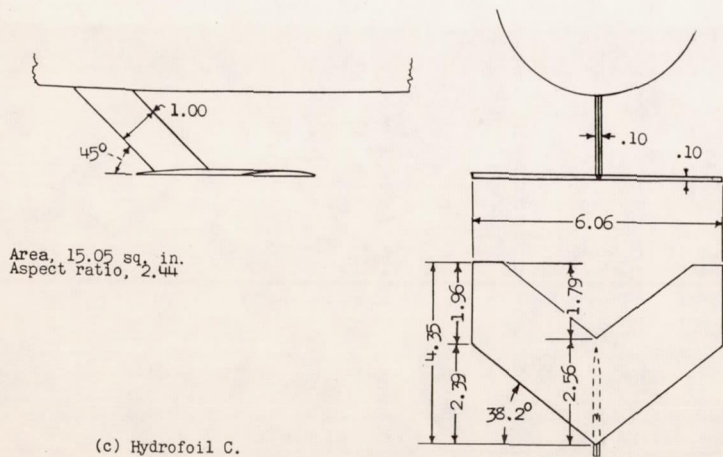
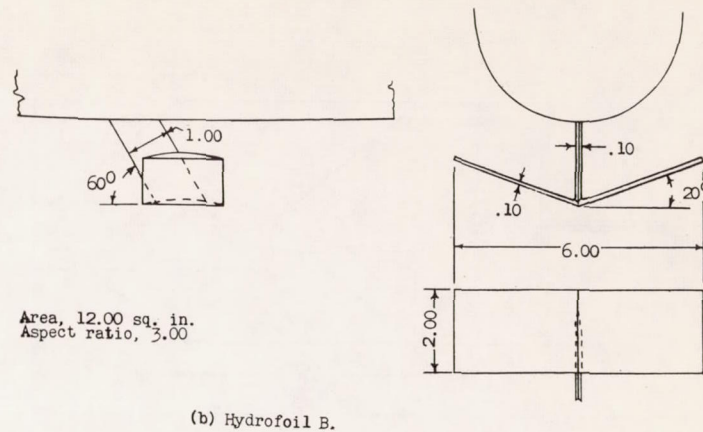
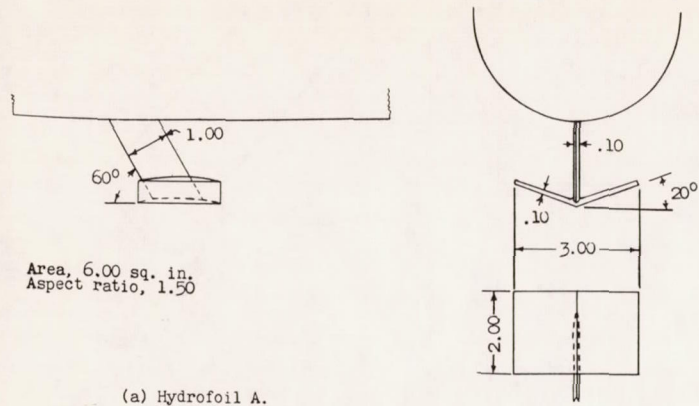
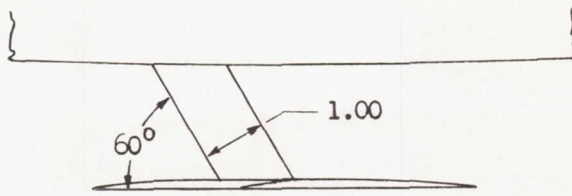
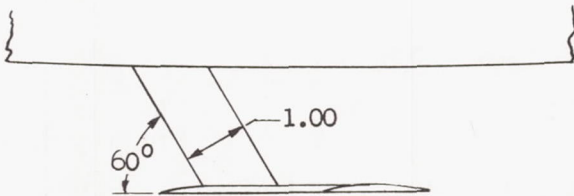
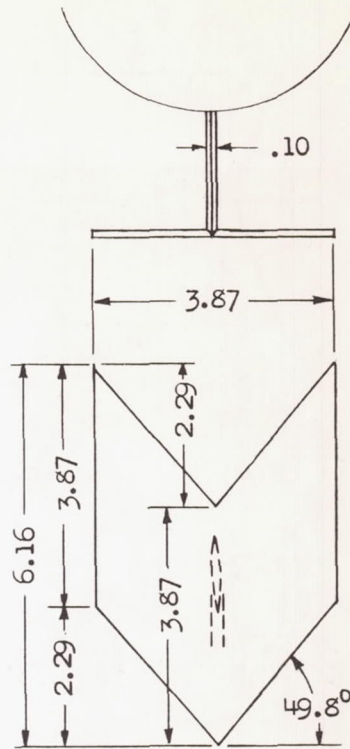


Figure 3.— Details of hydrofoils. (All dimensions are inches model-size, feet full-size.)

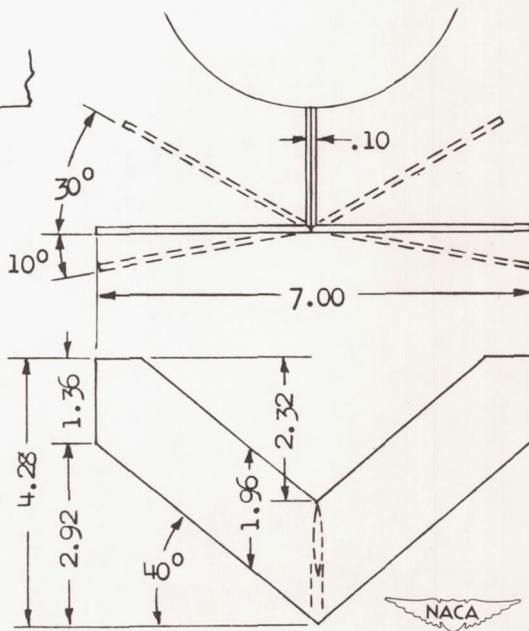


Area, 15.00 sq in.
Aspect ratio, 1.00

(e) Hydrofoil E.

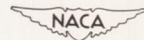


Dihedral	Area sq in.	Aspect ratio
30°	11.89	3.09
0°	13.71	3.57
-10°	13.51	3.52



(f) Hydrofoil F.

Figure 3.- Concluded.



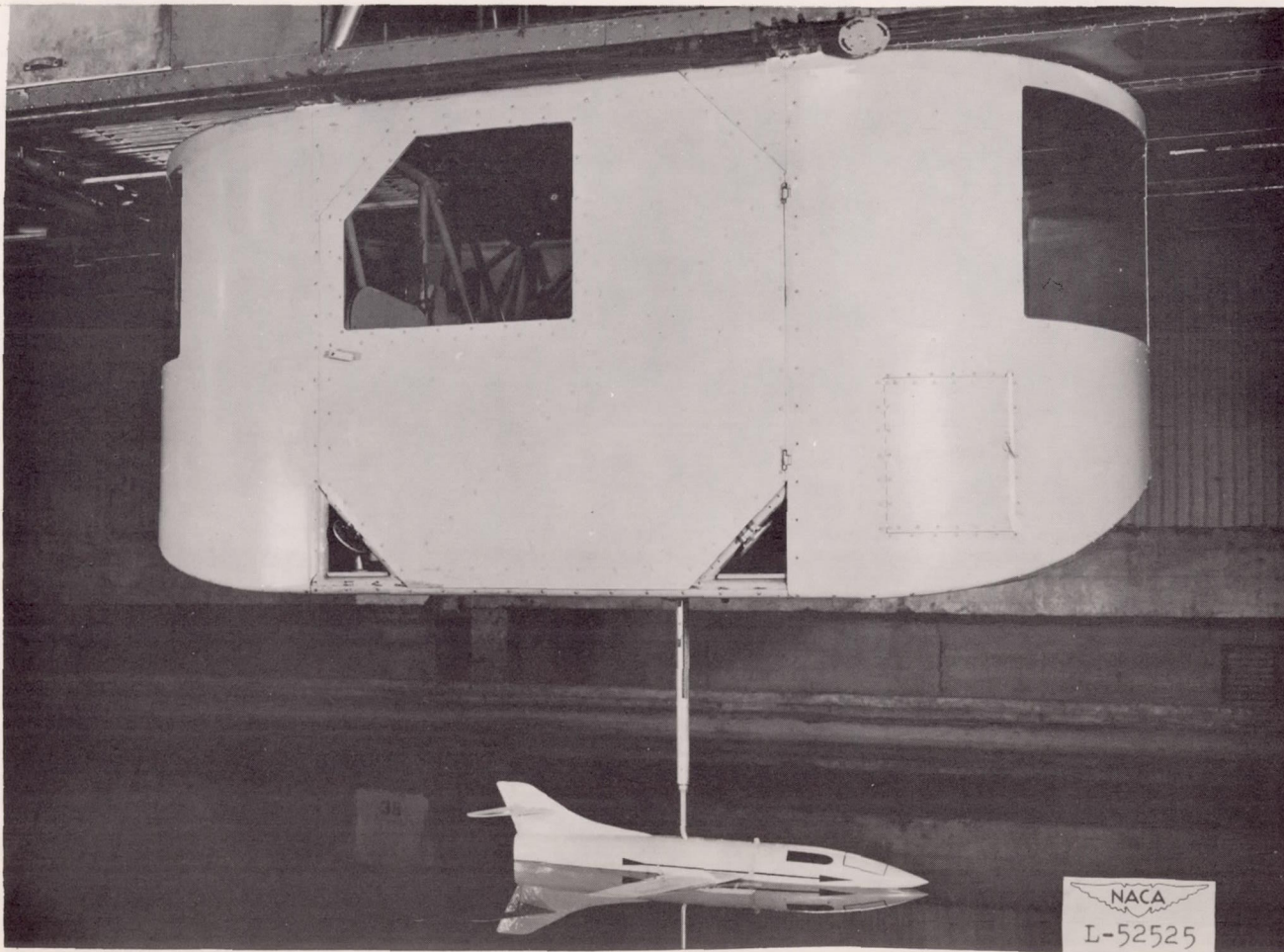
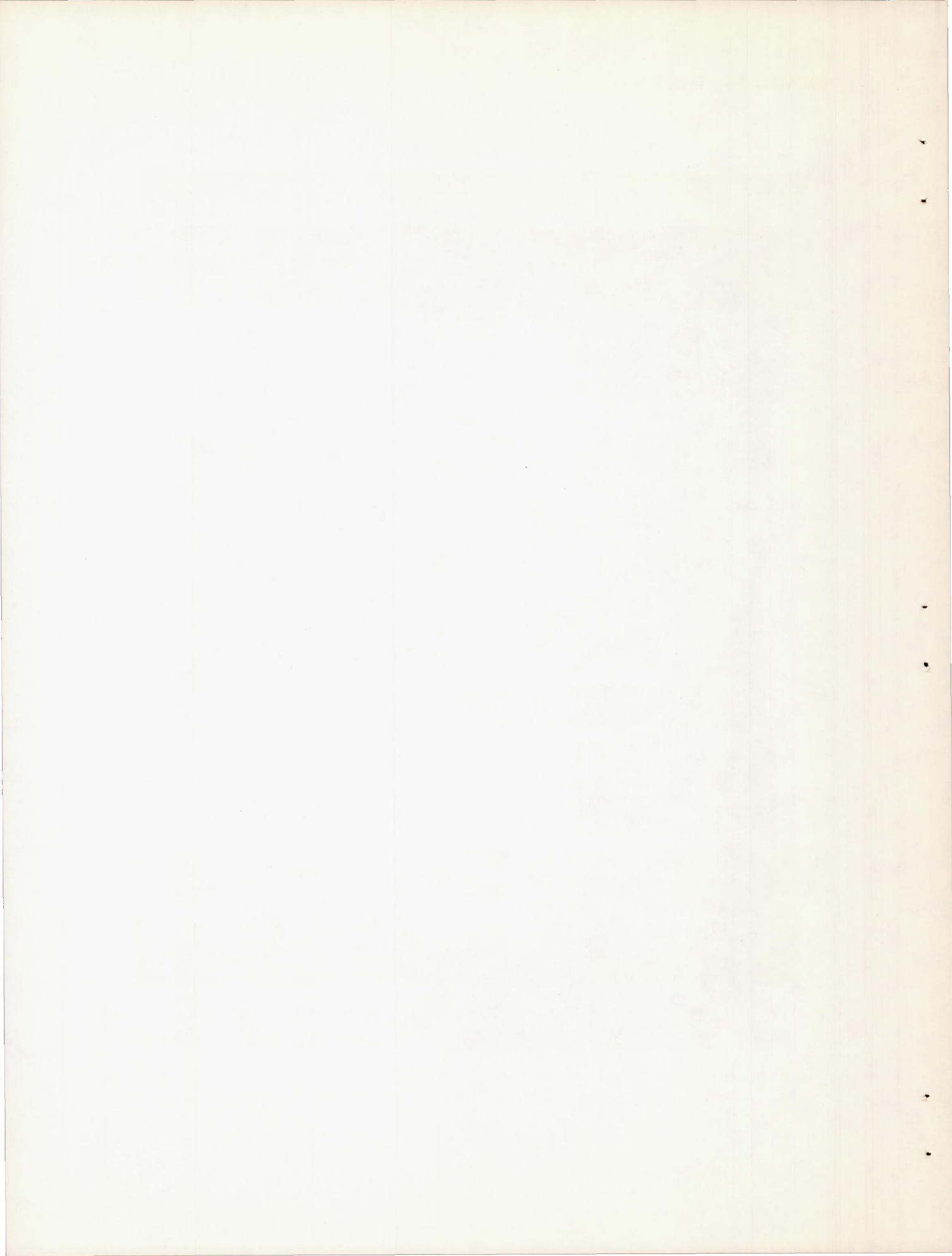
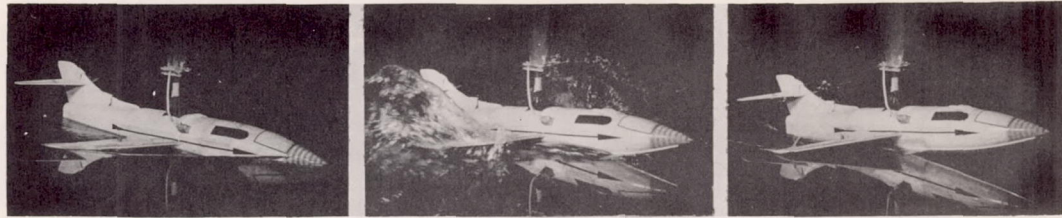


Figure 4.- Take-off test setup showing model floating at take-off weight.

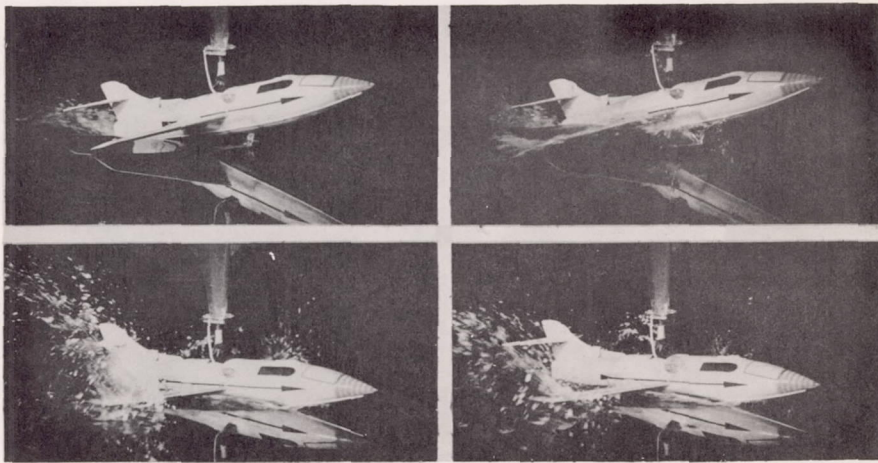




4

8

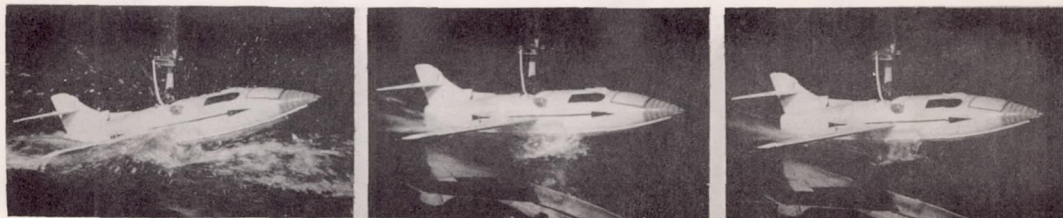
10



low and high positions of model during oscillatory motion of transition instability

11

13



15

30

40 fps model size

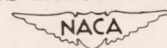
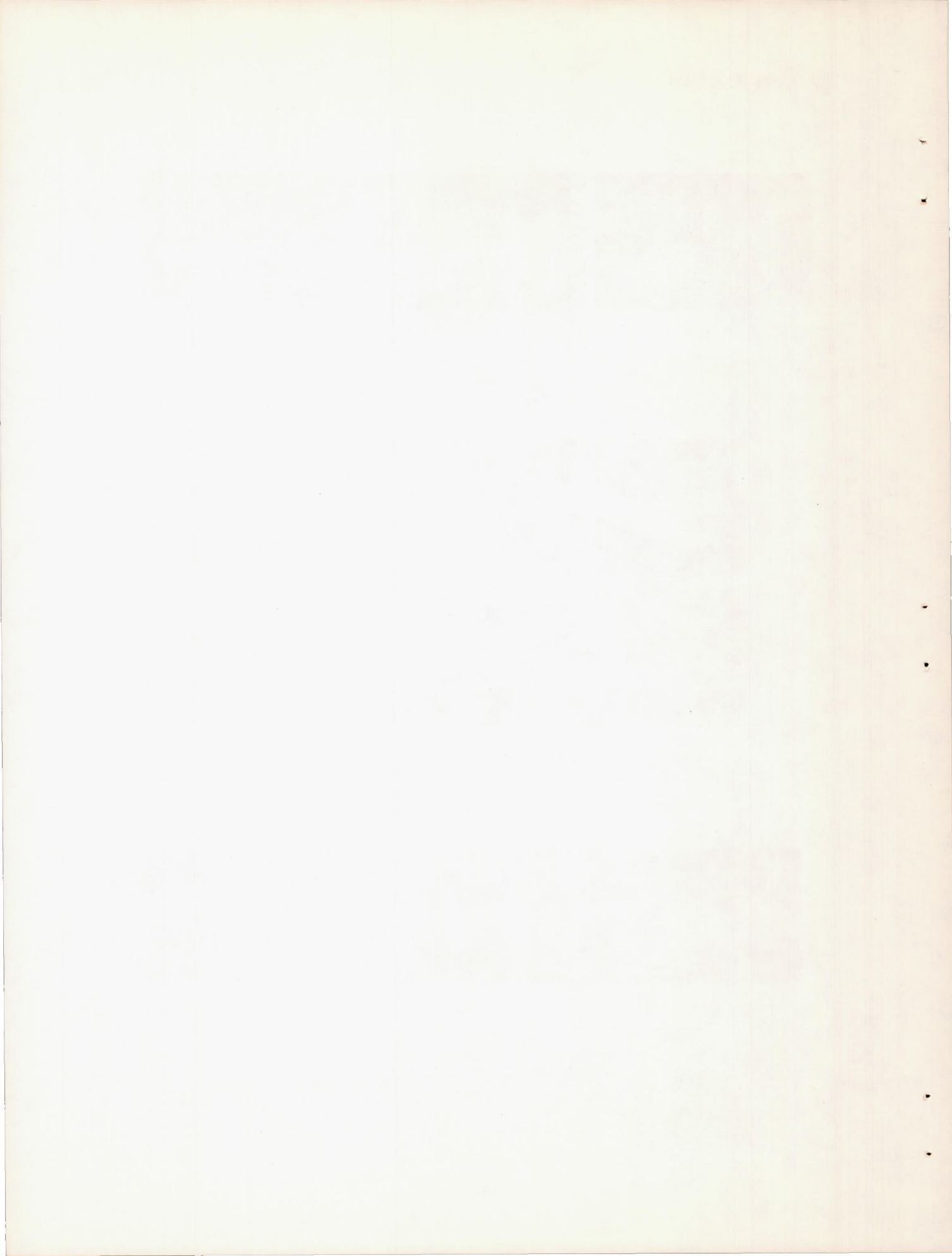
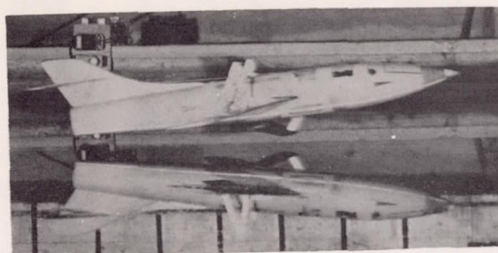


Figure 5.- Spray characteristics of model 229 with hydrofoil C. Pictures at 11 and 13 fps show two positions of model during transition instability.

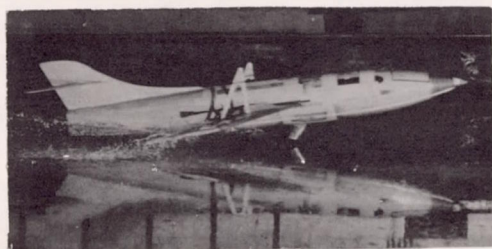




In flight
just before contact



1200 ft after contact



480 ft after contact



1400 ft after contact

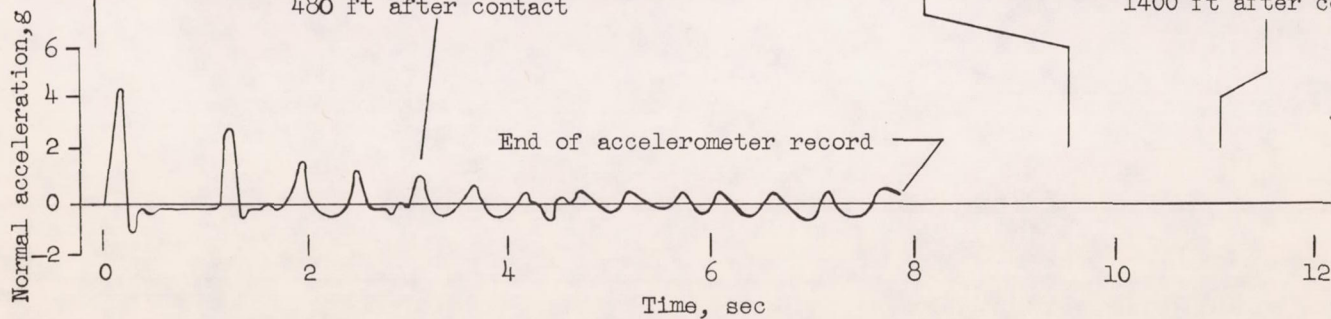


Figure 6.- Sequence photographs and time history of normal accelerations during typical landing of model 229 with 30° dihedral hydrofoil F. (All dimensions are full-size.)

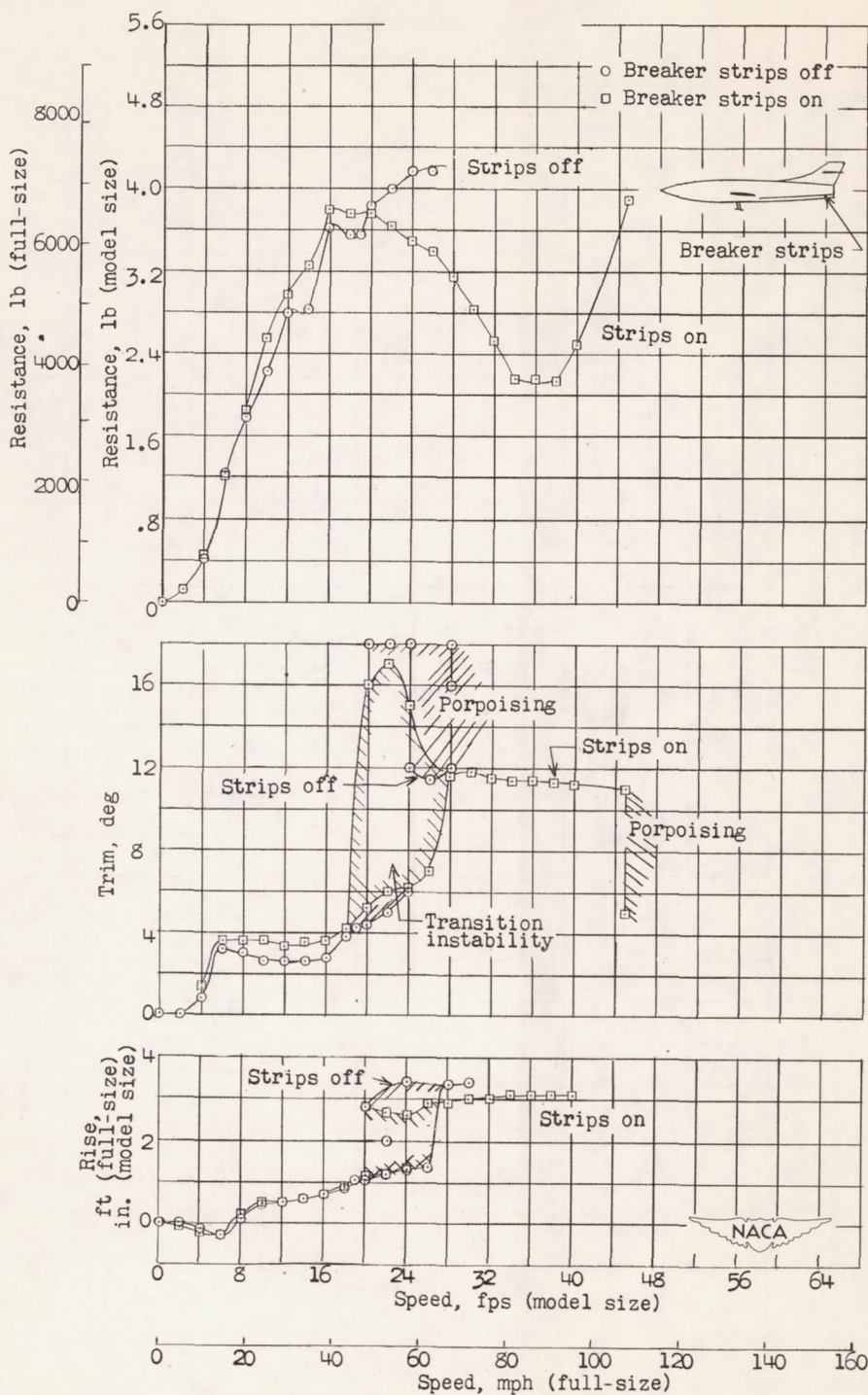


Figure 7.— Effect of breaker strips on take-off characteristics of model 229 with hydrofoil A. Hydrofoil position: longitudinal, X = 20 in.; vertical, Y = 4.5 in.; incidence, $i = 2^\circ$.

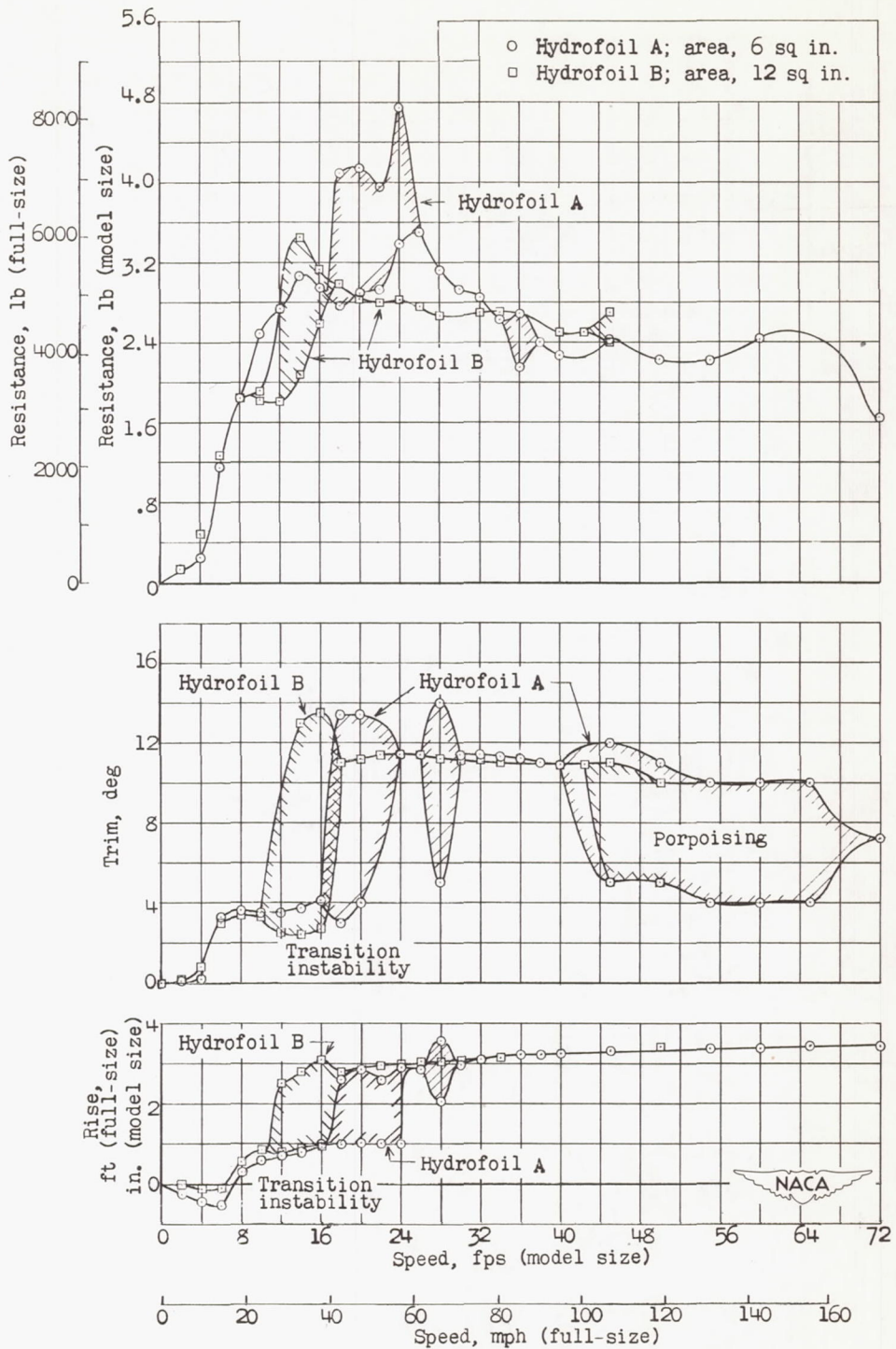


Figure 8.— Effect of hydrofoil area on take-off characteristics of model 229. Hydrofoils A and B. Hydrofoil position: longitudinal, $X = 20$ in.; vertical, $Y = 4.5$ in.; incidence, $i = 5^\circ$.

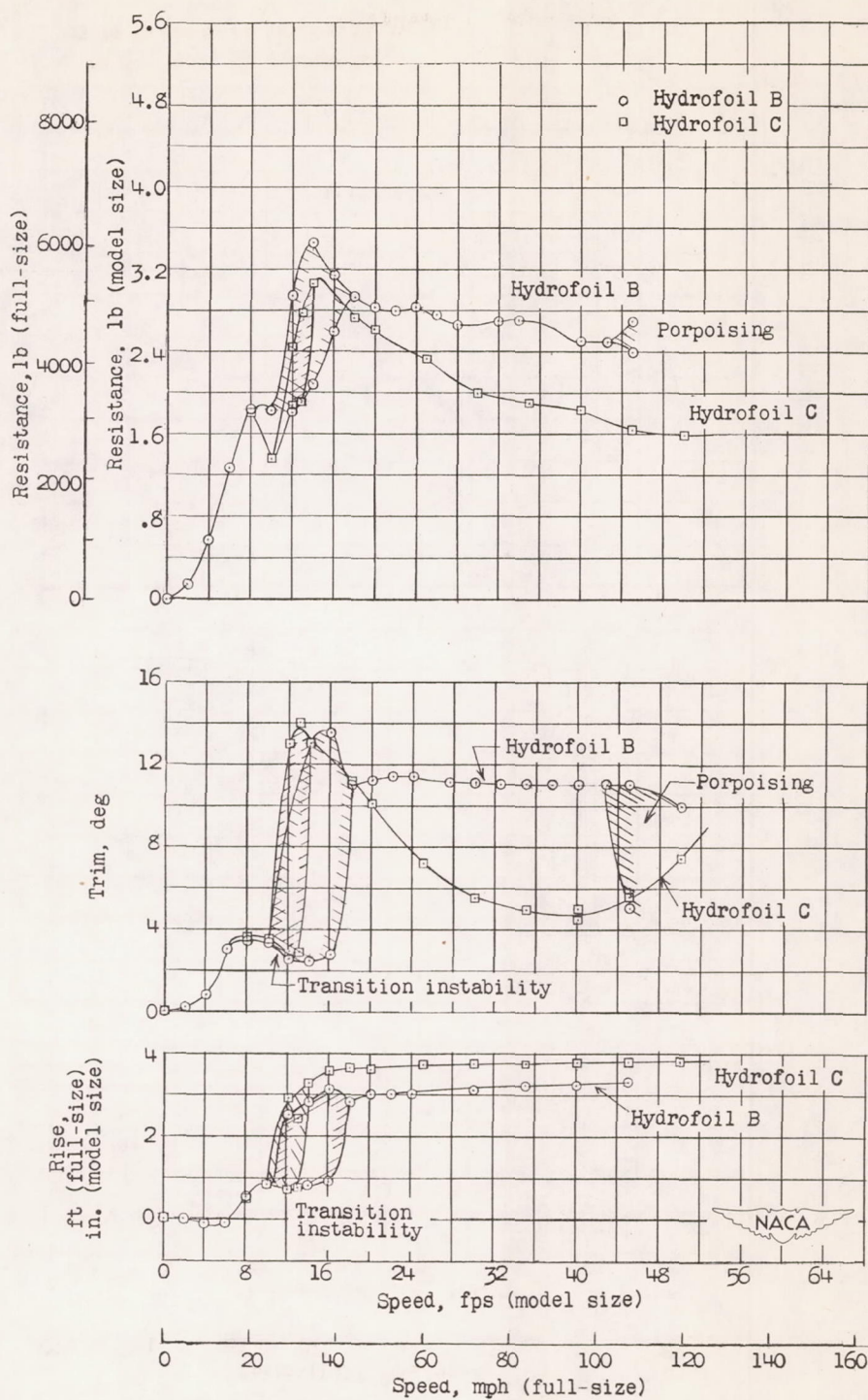


Figure 9.- Comparison of take-off characteristics of model 229 with hydrofoils B and C. Hydrofoil position: longitudinal, X = 20 in.; vertical, Y = 4.5 in.; incidence, $i = 5^\circ$.

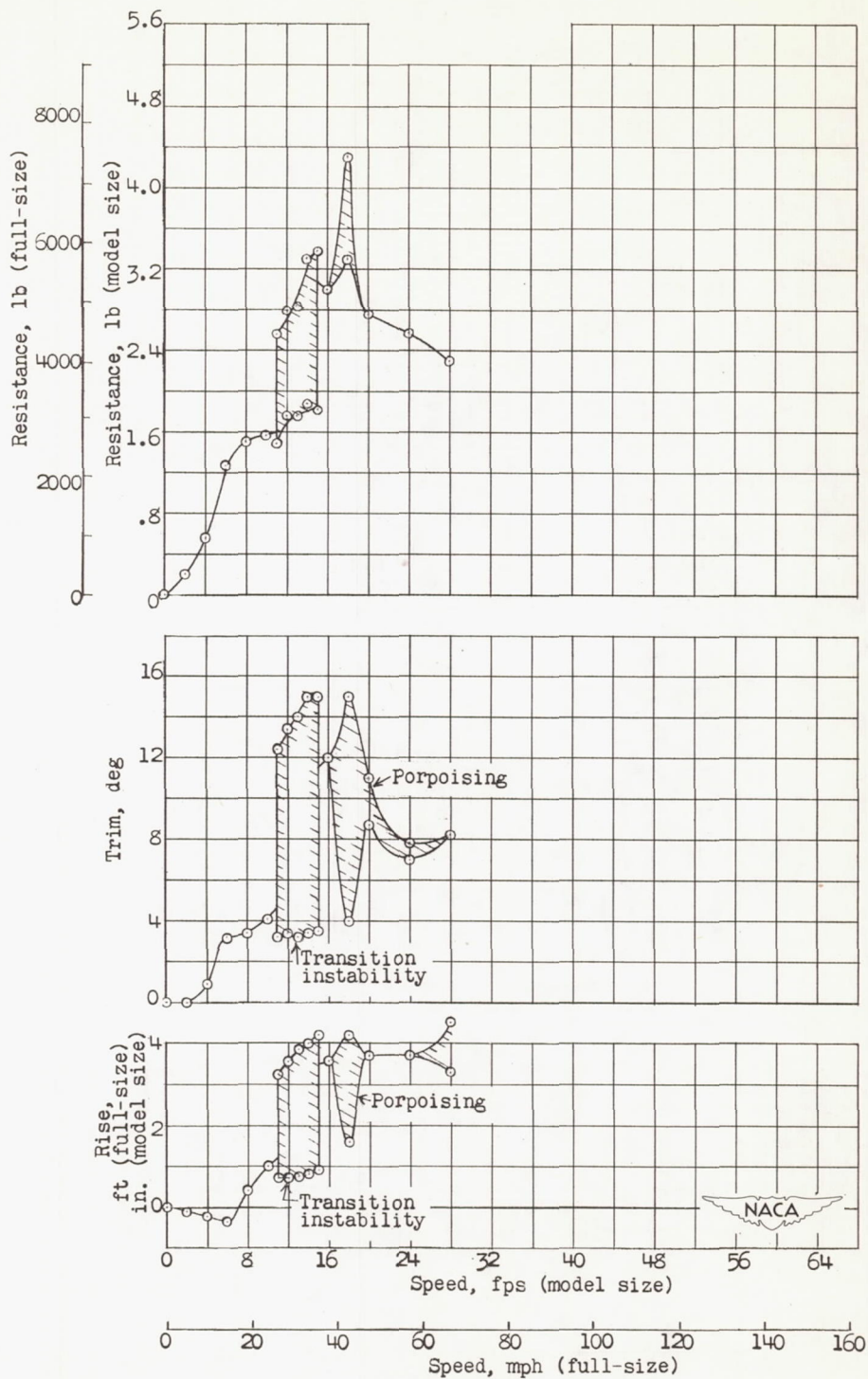


Figure 10.— Take-off characteristics of model 229 with hydrofoil D.
 Hydrofoil position; longitudinal, $X = 20$ in.; vertical, $Y = 4.5$ in.;
 incidence, $i = 5^\circ$.

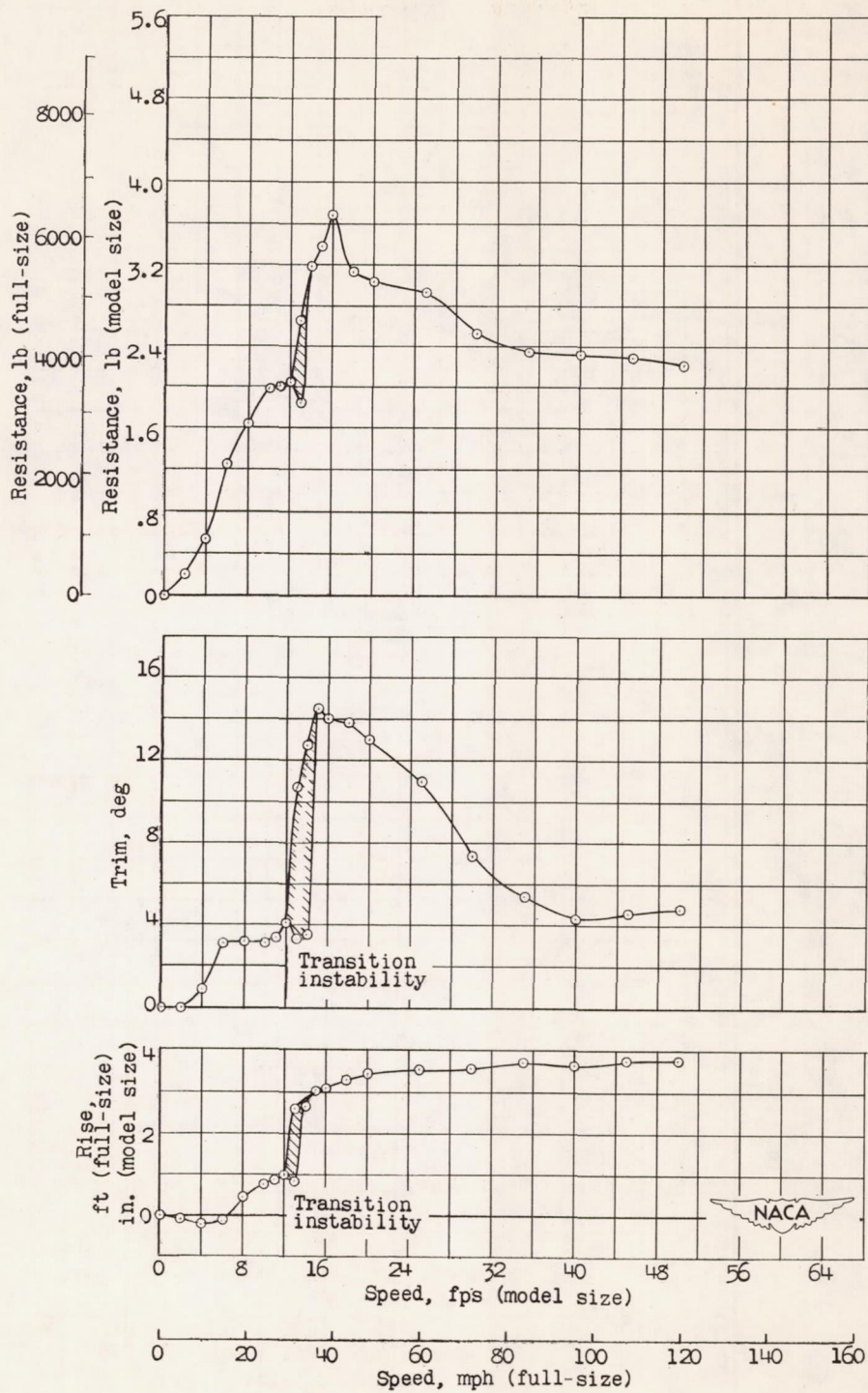


Figure 11.— Take-off characteristics of model 229 with hydrofoil E.
 Hydrofoil position; longitudinal, X = 20 in.; vertical, Y = 4.5 in.;
 incidence, $i = 5^\circ$.

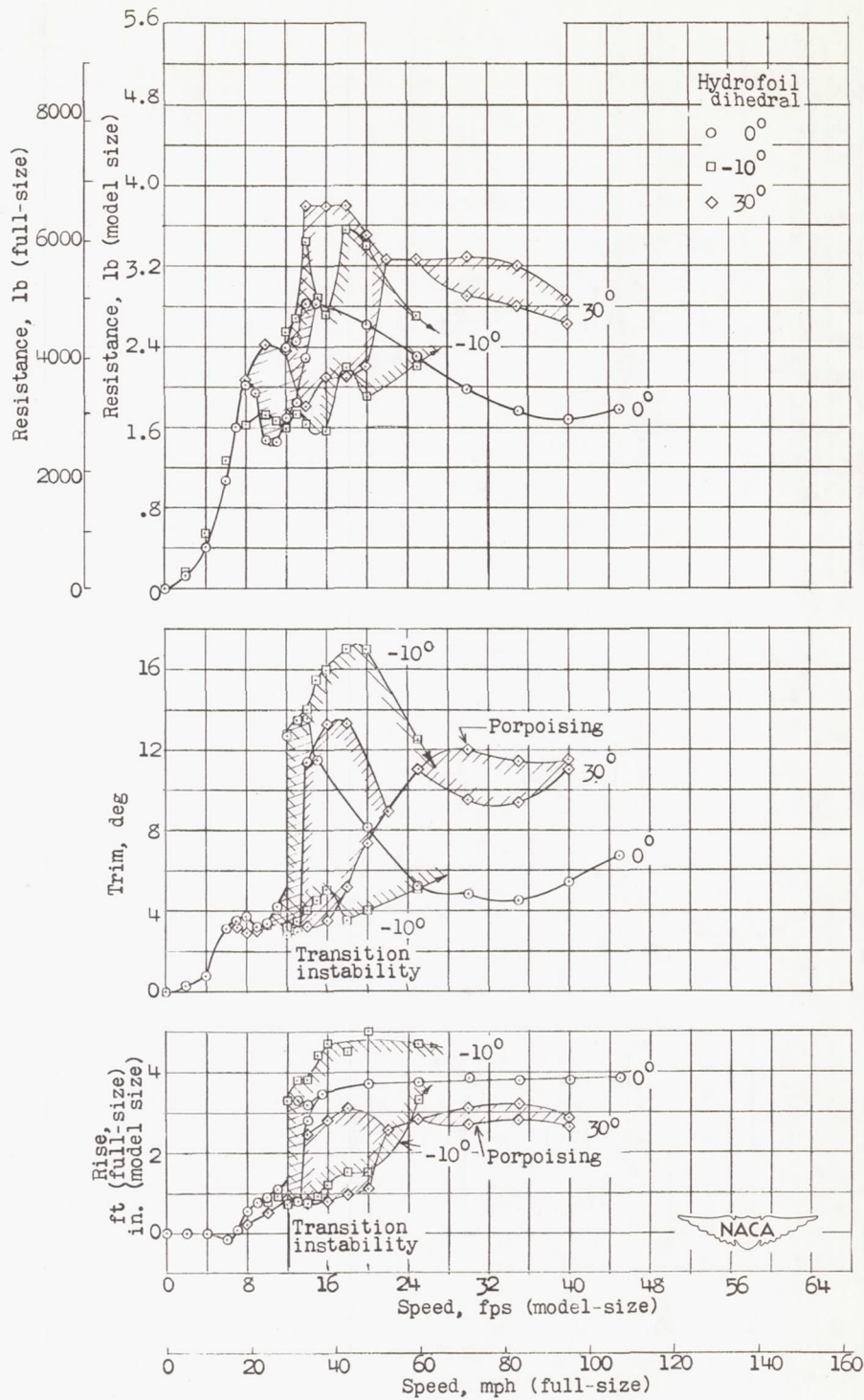
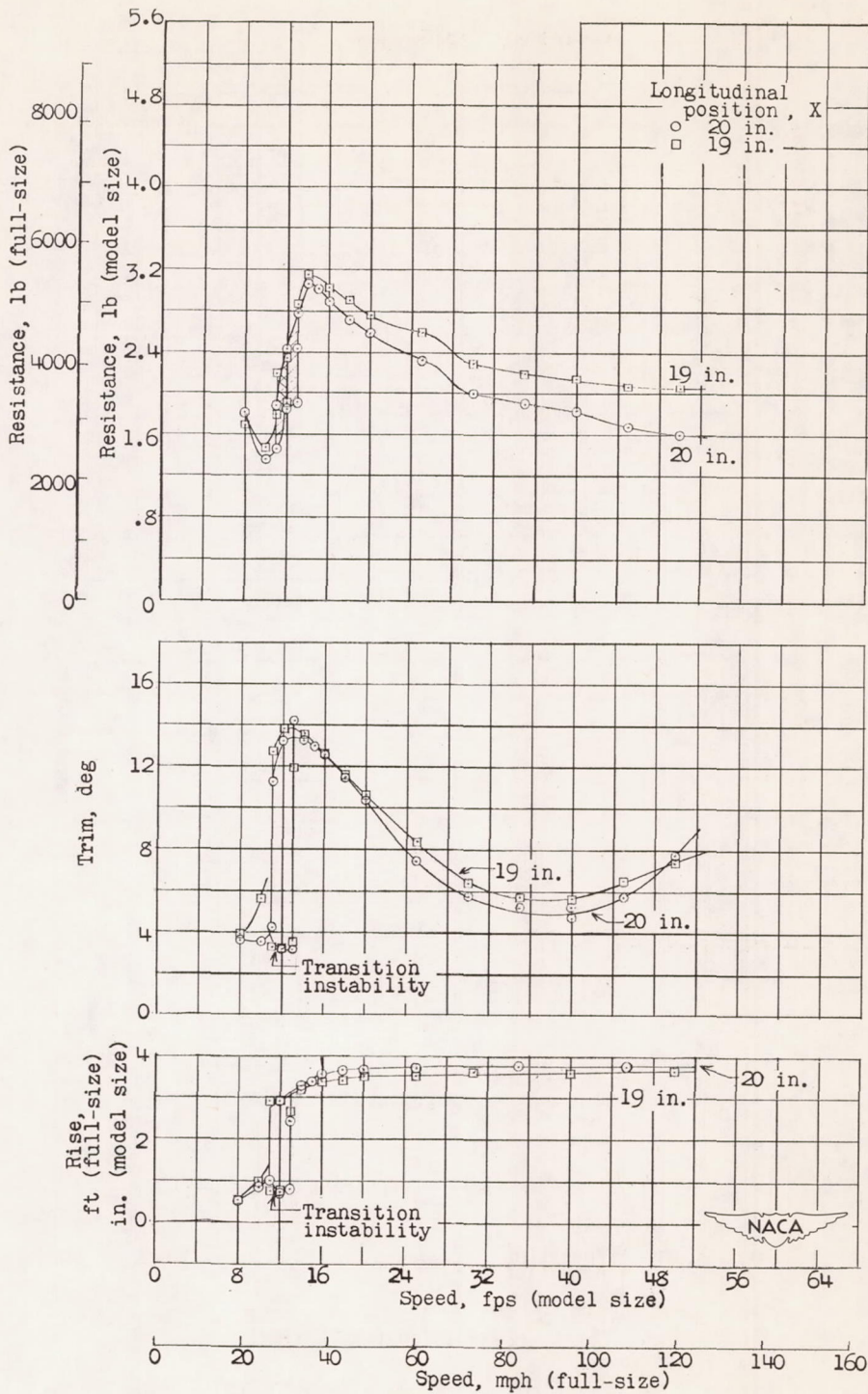
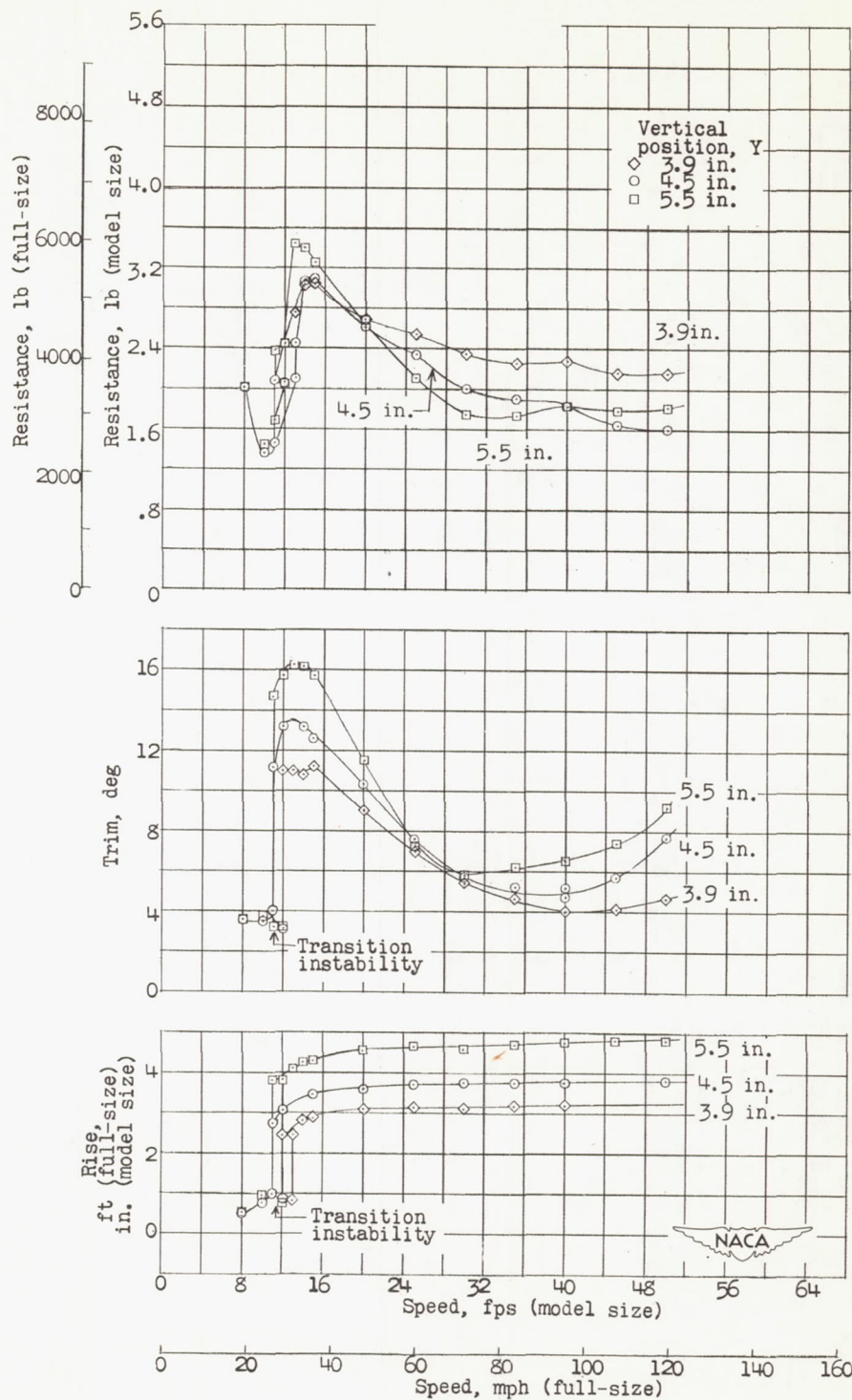


Figure 12.— Effect of hydrofoil dihedral on take-off characteristics of model 229 with hydrofoil F. Hydrofoil position; longitudinal, $X = 20$ in.; vertical, $Y = 4.5$ in.; incidence, $i = 5^\circ$.



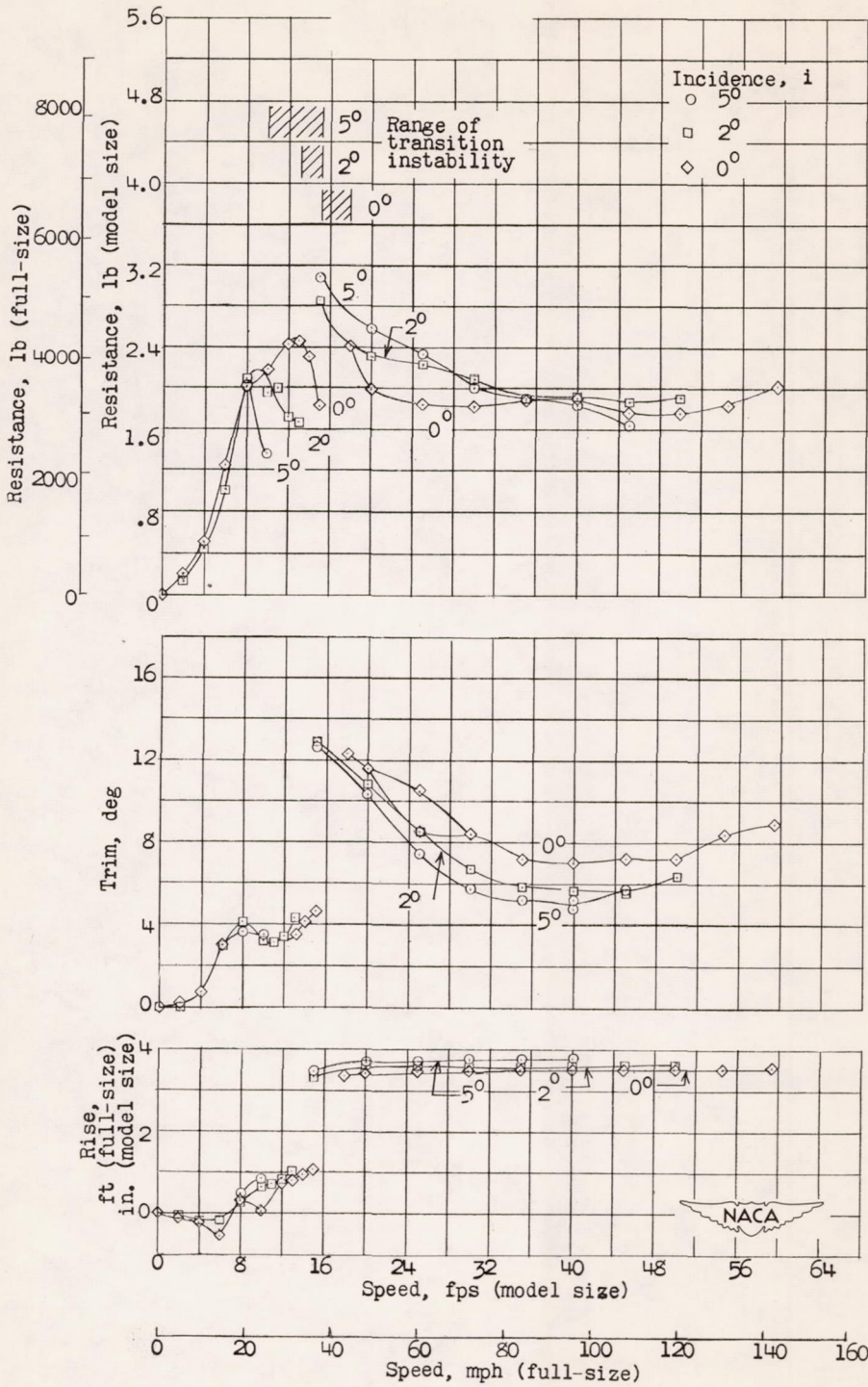
(a) Effect of longitudinal position. Vertical position, $Y = 4.5$ in.; incidence, $i = 5^\circ$.

Figure 13.- Effect of hydrofoil position on take-off characteristics of model 229 with hydrofoil C.



(b) Effect of vertical position. Longitudinal position, X = 20 in.; incidence, $i = 5^\circ$.

Figure 13.- Continued.



(c) Effect of incidence. Longitudinal position, X = 20 in.; vertical position, Y = 4.5 in.

Figure 13.- Concluded.